
Predicting Out-of-Domain Generalization with Local Manifold Smoothness

Nathan Ng

University of Toronto, Vector Institute
Massachusetts Institute of Technology

Neha Hulkund

Massachusetts Institute of Technology

Kyunghyun Cho

New York University
Prescient Design, Genentech
CIFAR Fellow

Marzyeh Ghassemi

Massachusetts Institute of Technology
CIFAR AI Chair, Vector Institute

Abstract

Understanding how machine learning models generalize to new environments is a critical part of their safe deployment. Recent work has proposed a variety of complexity measures that directly predict or theoretically bound the generalization capacity of a model. However, these methods rely on a strong set of assumptions that in practice are not always satisfied. Motivated by the limited settings in which existing measures can be applied, we propose a novel complexity measure based on the local manifold smoothness of a classifier. We define local manifold smoothness as a classifier’s output sensitivity to perturbations in the manifold neighborhood around a given test point. Intuitively, a classifier that is less sensitive to these perturbations should generalize better. To estimate smoothness we sample points using data augmentation and measure the fraction of these points classified into the majority class. Our method only requires selecting a data augmentation method and makes no other assumptions about the model or data distributions, meaning it can be applied even in out-of-domain (OOD) settings where existing methods cannot. In experiments on robustness benchmarks in image classification, sentiment analysis, and natural language inference, we demonstrate a strong and robust correlation between our manifold smoothness measure and actual OOD generalization on over 3,000 models evaluated on over 100 train/test domain pairs.

1 Introduction

As deep neural networks find increasing use in safety-critical domains such as autonomous driving [26] and healthcare [70], it is important to develop methods to understand how these models generalize to new environments. Although models have been shown empirically to generalize in many settings [27, 2, 51], they also exhibit numerous failure cases. For example, models have been shown to overfit to a dataset’s meta characteristics [60] or arbitrarily corrupted labels [75], learn spurious correlations [40], and change their predictions even with small adversarial perturbations [22, 57]. Many methods have been proposed to mitigate these issues, but precisely characterizing the generalization properties of a model in diverse settings remains an open problem.

Directly estimating the generalization of a trained model on test data is one approach to this problem [14, 32, 15, 19]. However, these methods are typically calculated based on the output predictive distribution of a model, which can become poorly calibrated in out-of-domain settings. Complexity measures are one potential set of tools to better fundamentally understand model generalization. Typically, these measures aim to theoretically bound generalization capacity [67, 5, 44, 51, 16, 50] or

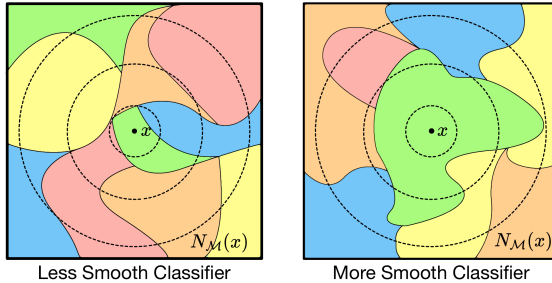


Figure 1: As the manifold neighborhood $N_M(x)$ around a test point x grows, the decision space is partitioned into a distinct set of decision regions. Smoother classifiers (right) have decision spaces that are less sensitive in this neighborhood and should generalize better compared to less smooth classifiers (left).

directly predict generalization [34, 39, 49, 64, 29], and are useful in reasoning about a model beyond its performance on a specific known test set. However, these methods often rely on a strong set of assumptions such as matching train/test distributions, labelled test data [64], access to model weights [50, 6, 52], model gradients [29], and training data [34]. In real world settings we are often given access only to a black box model and unlabeled data sampled from an unknown distribution. In these cases where it is potentially *more* important to have robust measures of model complexity, existing complexity measures cannot be used.

In this paper we propose a *local manifold smoothness* complexity measure that provides a generalization metric when existing complexity measures cannot be calculated. Our smoothness measure is defined as the sensitivity of a classifier’s output to local perturbations along the data manifold. We expect a smoother classifier that is less sensitive in this manifold neighborhood to generalize better than a less smooth classifier that is more sensitive in the same neighborhood. Empirically, we generate samples in the local manifold neighborhood using data augmentation, and define sensitivity as the fraction classified into the most commonly predicted class among these samples. Since our method depends only on the existence of a data augmentation method, it can be used in a wide range of experimental settings.

We investigate the correlation of a model’s local manifold smoothness with its capacity to generalize, defined as the model’s performance on unseen data. We focus on experimental settings with out-of-domain (OOD) dataset shifts [66], where test data is sampled from a distribution different from the training distribution. We select common OOD benchmarks in image classification [38, 43, 59, 13, 12, 48, 4], sentiment analysis [55], and natural language inference [71] and train a large pool of over 3,000 models with varying architectures and generalization properties on these datasets. Generating samples using well-established data augmentation methods [54, 11, 69, 73] for each task and data domain, we evaluate the quality of our measure on over 100 pairs of training/test domains.

Specifically, given a pool of models trained with data from a single training domain, we evaluate the correlation of our measure with generalization on in-domain data ($ID\tau$) and out-of-domain data (Micro/Macro τ). In settings where we have access to additional labeled test data from other domains and can make direct predictions of OOD generalization, we evaluate the Pearson R^2 and mean absolute error of these predictions. Finally, we evaluate the correlation of models trained with different architectures (Arch τ) as well as on extreme OOD data from specialized domains. We find that our smoothness measure outperforms baselines in all combinations of experimental setting and evaluation metrics, save one. To our knowledge, our measure is the only complexity measure that is applicable in common machine learning robustness evaluation settings, and provides the first analysis of a complexity measure in natural language tasks as well as OOD settings.

2 Related Work

Measures of Complexity Traditional methods of analyzing the generalization bounds of neural networks use theoretical measures of complexity. VC dimension [67] and Rademacher complexity [5] measure the capacity of a particular function class and give bounds on their generalization error, although they are often vacuous at the scale of deep neural networks [16]. Another set of analyses use the PAC-Bayes framework [44, 51, 16, 20] in order to build tighter generalization bounds by considering the “sharpness” of the local minima. Norm-based measures [50, 6, 52]

bound generalization by considering different norms of the weights of learned networks. More recent analyses of complexity have focused on empirically motivated measures that do not provide theoretical bounds. These include the sharpness of minima in parameter space [34], Fisher-Rao norm [39], distance from initialization [47], path norm [49], layer margin distributions [29], and perturbation response curves [64]. Most similar to our method is Aithal K et al. [1], who use robustness to augmentations as a complexity measure. However, their method requires access to labelled data, which we assume we do not have.

Predicting Generalization Recent work has focused on correlating these complexity measures with and directly predicting in-domain generalization [31]. However, in real world settings, test distributions often differ from training distributions [37]. Although some generalization bounds have been derived for these OOD settings [20, 7, 76], they rely on access to the test data distribution. A separate line of work departs from complexity measures altogether and directly predicts OOD generalization from unlabelled test data. These methods either predict the correctness of the model directly on individual examples [14, 32, 15] or directly estimate the total error [19, 24, 9, 10, 68]. Although these methods work well in practice, they do not provide any insight into the underlying mechanism of generalization since they act only on the output layer of the network.

Measuring Function Smoothness The simplest way to measure the smoothness of a function $f : \mathcal{X} \rightarrow \mathcal{Y}$ is through its differentiability class. However, this is not a very useful inductive bias for a model since differentiability is very local and metric dependent. One alternative measure is Lipschitz continuity. Enforcing this property on neural networks is commonly done by restricting the learned function class with spectral regularization [74], spectral normalization [45], and other norm based regularization methods on layer weights [6, 51, 18]. Other methods regularize the the norm of gradients with respect to the the inputs of the network [17, 3, 25]. A key component of smoothness regularization is *where* and *how* it is enforced. Enforcing global properties such as Lipschitz continuity in regions where there is no data can restrict the learned function unnecessarily [63]. In addition, if the data lies on a low-dimensional manifold, then our smoothness should only be regularized with respect to this manifold, rather than the entire input space.

3 Manifold Smoothness Measure

In this section we introduce our manifold smoothness measure. We start by motivating our local smoothness definition, then describe how our measure is estimated in practice using samples from a neighborhood distribution. Finally we describe how we evaluate the quality of our measure.

3.1 Motivation

Consider a classification task from an input space \mathcal{X} to an output space \mathcal{Y} with k classes. We are given a model $f : \mathcal{X} \rightarrow \mathcal{Y}$ trained on an in-domain training dataset $\mathcal{D}_i = \{(x_i^1, y_i^1), \dots, (x_i^n, y_i^n)\}$ sampled from a distribution $P_i(\mathcal{X}, \mathcal{Y})$, and an out-of-domain test dataset $\mathcal{D}_o = \{(x_o^1, y_o^1), \dots, (x_o^m, y_o^m)\}$ sampled from a distribution $P_o(\mathcal{X}, \mathcal{Y})$. We assume points in both datasets concentrate around a lower dimensional manifold \mathcal{M} [8]. Consider a point $x \in \mathcal{D}_o$ that belongs to class j . We define the manifold neighborhood $N_{\mathcal{M}}(x, r)$ as the set of points in \mathcal{M} that are at most a distance r away from x as measured in the original input space \mathcal{X} . As r increases, the decision space within $N_{\mathcal{M}}$ becomes partitioned into a set of distinct decision regions for each class. For a given r , we define the neighborhood decision distribution as

$$p_j(x) = \frac{|\{x' \in N_{\mathcal{M}} : f(x') = j\}|}{|N_{\mathcal{M}}|}, \quad (1)$$

and define our smoothness measure as

$$\mu(f, x) = \max_{j \in \mathcal{Y}} p_j(x). \quad (2)$$

Intuitively, this measure captures the sensitivity of a classifier’s output within the manifold neighborhood of x . As shown in Figure 1, a smoother classifier will be less sensitive and will predict the same class for most of the points in the neighborhood. In contrast, a less smooth classifier will be more sensitive and will predict different classes for different points in the neighborhood.

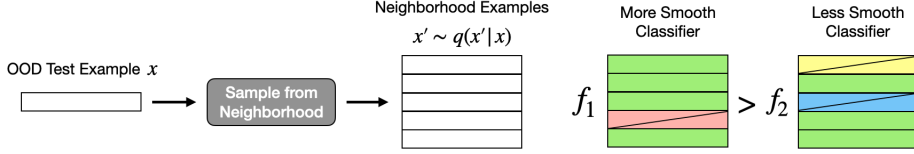


Figure 2: To estimate our smoothness measure we generate a set of nearby examples for every test example using a neighborhood distribution q . This set of examples is then evaluated using each classifier. We expect classifiers with more sampled points classified in the most common class to generalize better to the given test set.

As an alternative to our proposed definition of smoothness, we also consider the negative entropy of the neighborhood decision distribution $\sum_{j=1}^k p_j(x) \log(p_j(x))$, but find that it performs similarly or slightly worse than our proposed definition. Full results on this alternative definition of smoothness are presented in the appendix in Table 6.

3.2 Estimating Neighborhood Smoothness

Calculating our smoothness measure exactly is intractable since we do not have access to the true manifold \mathcal{M} . Instead, we assume access to a conditional distribution $q(x'|x)$ from which we can sample points from the manifold neighborhood $N_{\mathcal{M}}(x) = \{x' \sim q(x'|x)\}$. In this paper we consider distributions $q(x'|x)$ defined by data augmentation transformations. We modify the size of the neighborhood by making $q(x'|x)$ more or less noisy. We estimate our smoothness measure for a given point x as the fraction of points sampled from $q(x'|x)$ classified as the dominant label

$$\mu(f, x) = \mathbb{E}_{x' \sim q(x'|x)} \mathbb{1}(f(x') = \hat{y}(f, x)), \quad (3)$$

where

$$\hat{y}(f, x) = \arg \max_{j \in \mathcal{Y}} \mathbb{E}_{x'' \sim q(x''|x)} \mathbb{1}(f(x'') = j) \quad (4)$$

is the dominant label. The average smoothness across the entire dataset \mathcal{D}_o is then $\frac{1}{m} \sum_{j=1}^m \mu(f, x_o^j)$. Since exactly calculating the expectation in Eqns. 3 and 4 is intractable, we estimate it as shown in figure 2. For a given test example x , we first generate n samples from the neighborhood distribution $q(x'|x)$. Next, we evaluate the classifier at each sampled point x' and calculate \hat{y} as the most commonly predicted class. μ is then the fraction of sampled points that our classifier labels as \hat{y} .

Our smoothness measure is simple to calculate and makes no assumptions about the model or the distribution from which test data was sampled. In addition, since our measure relies only on the augmentation method $q(x'|x)$ chosen and does not use labels from the test data, it is applicable in many settings where existing complexity measures cannot be calculated, including common robustness evaluation settings.

3.3 Evaluation Metrics

Given a set of domains defined by distributions $\{P_1, P_2, \dots, P_n\}$ and a set of datasets $\{\mathcal{D}_i \sim P_i\}_{i=1}^n$ sampled from these domains, we train a set of models $F_i = \{f_i^1, f_i^2, \dots, f_i^m\}$ on each dataset \mathcal{D}_i . We evaluate all models $f_i^k \in F_i$ on all OOD test datasets $\mathcal{D}_o : o \neq i$, generating a set of smoothness and generalization values (μ_{io}^k, g_{io}^k) . We define generalization as the top-1 accuracy of f_i^k on \mathcal{D}_o .

We evaluate our measure first by predicting the generalization of a given model to an OOD test set. Specifically, we select an OOD test set \mathcal{D}_o and an in-domain training set $\mathcal{D}_i : i \neq o$ and predict the OOD generalization g_{io}^k of a model f_i^k trained on \mathcal{D}_i and evaluated on \mathcal{D}_o from its smoothness value μ_{io}^k . To generate these predictions we use a linear model $\hat{g} = a\mu + b$ where $a, b \in \mathcal{R}$ are the parameters of our model. To estimate our parameters a and b , we select a pool of models $\{f_j^k \in F_j : j \neq i, o\}$ that are trained on all remaining datasets. Each model f_j^k in this pool is evaluated on the OOD dataset \mathcal{D}_o to give us a set of pairs $\{(\mu_{jo}^k, g_{jo}^k)\}$. We then find a, b by minimizing the mean squared error $(a^*, b^*) = \arg \min_{a, b} \sum_{j, k} (a\mu_{jo}^k + b - g_{jo}^k)^2$ on all models in the pool.

We use the learned parameters to make generalization predictions $\hat{g}_{io}^k = a\mu_{io}^k + b$ for every model $f_i^k \in F_i$ on \mathcal{D}_o and measure the coefficient of determination R^2 [21]. We also measure the residuals of our linear model by calculating the mean absolute error (**MAE**) between our predictions and the actual generalization. For every pair of training domain i and OOD test domain o , we evaluate R^2 and MAE then average each metric across all pairs.

We also consider the rank correlation between our smoothness measure and actual generalization. Specifically, for a pair of models f_i, f_j with measure and generalization pairs (μ_i, g_i) and (μ_j, g_j) , we want $g_i > g_j$ if $\mu_i > \mu_j$. We use Kendall’s rank τ coefficient [33] to measure how consistent these sets of rankings are. We measure four different τ values:

ID τ This metric evaluates the correlation of our measure with in-domain generalization. We select a training dataset \mathcal{D}_i and consider pairs $\{(\mu_{ii}^k, g_{ii}^k)\}$ generated from the set of models F_i trained on \mathcal{D}_i . τ values are averaged across all training domains.

Macro τ This metric evaluates the correlation of our measure individually on each training/OOD test domain pair. We select a training dataset \mathcal{D}_i and a OOD test dataset \mathcal{D}_o and consider pairs $\{(\mu_{io}^k, g_{io}^k)\}$ generated from the set of models F_i trained on \mathcal{D}_i . τ values are averaged across all pairs of training and OOD test domains.

Micro τ This metric evaluates the correlation of our measure on a given OOD test domain across models trained on all other domains. We select a single OOD test domain \mathcal{D}_o and consider pairs $\{(\mu_{io}^k, g_{io}^k)\}$ generated from the set of models $\{f_i^k \in F_i : i \neq o\}$ trained on all other datasets $\{D_i : i \neq o\}$. τ values are averaged across all test domains.

Arch τ This metric evaluates the correlation of our measure on models trained with different architectures. Arch τ is calculated similar to Micro τ , except F_i now includes models from all architectures. τ values are averaged across all test domains.

4 Experimental Setup

Empirically evaluating the quality of a complexity measure is difficult and requires careful experimental design. Typically, evaluation is done by generating a large pool of models with sufficiently varied generalization properties, but if we generate these models by varying only a few hyperparameters, our observed correlation may be an artifact of these factors affecting both generalization and our measure. To this end, we follow a similar experimental setup to Jiang et al. [30].

4.1 Data

For our experiments we focus on three tasks: image classification as well as sentiment analysis on single sentences and natural language inference on sentence pairs.

Image Classification For image classification we construct two sets of domains, one comprised of CIFAR10 [38], CINIC10 [12], CIFAR10.1[59], and CIFAR10.2[43], as well as one comprised of SVHN [48], MNIST [13], and Colored MNIST [4]. Domains in each set share the same set of output classes.

Sentiment Analysis (SA) We use the Amazon reviews dataset [55] which contains product reviews from Amazon. Following Hendrycks et al. [28] and Ng et al. [54], we split the dataset into 10 different domains based on review category. For all domains and datasets, models are trained to predict a review’s star rating from 1 to 5.

Natural Language Inference (NLI) We use the MNLI [71] dataset, a corpus of NLI data from 10 distinct genres of written and spoken English. We train on the 5 genres with training data and evaluate on all 10 genres. Models are given two sentences, a premise and hypothesis, and predict whether the hypothesis is entailed by, is neutral to, or contradicts the premise.

4.2 Defining the Neighborhood

There are many different ways to define the neighborhood distribution $q(x'|x)$ from which we sample. Each choice implicitly also defines the underlying manifold with respect to which we measure

Model	Dataset	Training Domain	Batch Size	Depth	Width	Dropout	Weight Decay	Label Noise	Learning Rate	Batch Norm	# Trained	# Converged
CNN	Amazon	10	3	3	3	2	3	—	—	—	1620	1613
	MNLI	5	3	3	3	2	—	3	—	—	910	796
RoBERTa	Amazon	10	3	—	—	2	3	3	—	—	540	332
	MNLI	5	3	—	—	2	3	3	—	—	270	213
NiN	SVHN	—	3	3	—	3	2	—	—	—	54	54
VGG	CIFAR10	—	2	2	2	2	2	—	—	—	32	32
	CIFAR10	—	3	3	—	3	2	—	—	—	54	54
CNN	CINIC10	—	2	2	4	—	2	—	2	2	128	128

Table 1: Number of possible hyperparameter values for each architecture and task. Fields denoted with a — indicate that this hyperparameter is fixed or not applicable. We also list the total number of models trained and converged in each model pool. In total we evaluate 3,222 models.

smoothness. One natural choice is to utilize data augmentations, since these are transformations over which we want our classifiers to be smooth.

We compare two methods for data augmentation for image classification: RandAugment [11] and random patch erasing [77]. We call smoothness measures based on these three augmentations **MS-Rand** and **MS-Erase** respectively. We also consider three methods for data augmentation on natural language: SSMBA [54], EDA [69], and backtranslation (BT) [61, 73]. We call smoothness measures based on these three augmentations **MS-SSMBA**, **MS-EDA**, and **MS-BT** respectively. For all experiments we generate $n = 10$ samples for each example, although ablations in section 5.3 show that our method is relatively robust to the specific number of samples generated. We provide further details on implementations and noise levels for all methods in the Appendix A.5.

4.3 Model and Hyperparameter Space

For image classification, we use models trained for the Predicting Generalization in Deep Learning competition (PGDL) [31]. We select models from tasks 1, 2, 4, 5, and 9, which covers Network in Network (NiN) [41], VGG [65], and CNN models trained on CIFAR10, CINIC10, and SVHN. On natural language tasks we consider CNN [35] and RoBERTa [42] based models. We modify the CNN model to make predictions on sentence pairs by generating a representation for each sentence independently, then concatenating the two representations, their difference, and element-wise product before classification [46]. Following Jiang et al. [30], we consider varying the following hyperparameters: training domain, batch size, depth, width, dropout, and weight decay.

We consider an additional hyperparameter of label noise, which we apply by randomly replacing a fraction of training labels with uniform samples from the label space. We argue that label noise is not an artificial training setting as stated in [30] but rather a method of entropy regularization [58, 72] which prevents models from becoming overconfident and decreases smoothness. We find that label noise is necessary to achieve a wide enough range of model generalizations for most of our experiments. Details on hyperparameter variations for each task and model are provided in Table 1.

In order to control for the varying convergence rates and learning capacities of our different models, we follow [30] and early stop the training of models when they reach a given training cross entropy loss (usually around 99% training accuracy), or if they reach the max number of training epochs. We discard all models which do not converge within this time. The total number of models trained and converged in each pool is provided in Table 1. We include further details on model training, the hyperparameter space, and specific choices in hyperparameters in Appendix A.4, A.2, and A.3.

4.4 Baselines

As a baseline comparison against our selected neighborhood distributions, we consider horizontal flips and crops for image classification and random replacement on a percentage of tokens for natural language tasks. We call these baselines **MS-FC** and **MS-RandAug**. Since our experimental setting makes so few assumptions, there are very few complexity measures that we can compare against. We consider complexity measures that require only model weights, specifically the **Spectral** [74, 52] and **Frobenius** [50] norms. However, in our experiments we find close to 0 or negative correlation for these measures, so we do not report their performance.

Measure	R^2	MAE	Macro τ	Micro τ	ID τ	Arch τ
MS-RandAug	0.892	3.97	0.750	0.650	0.792	0.794
MS-Erase	0.303	5.97	0.205	0.107	0.304	0.249
MS-FC	0.361	6.03	0.202	0.107	0.260	0.671
ATC-NE	0.625	4.44	0.536	0.578	0.707	0.689
ATC-MC	0.629	4.38	0.542	0.578	0.692	0.685

(a) Results on image classification.

Measure	CNN					RoBERTa					
	R^2	MAE	Macro τ	Micro τ	ID τ	R^2	MAE	Macro τ	Micro τ	ID τ	Arch τ
MS-SSMBA	0.662	1.93	0.677	0.689	0.629	0.972	1.29	0.832	0.829	0.838	0.588
MS-EDA	0.641	2.04	0.664	0.649	0.611	0.968	1.45	0.830	0.810	0.830	0.512
MS-BT	0.550	2.99	0.592	0.501	0.538	0.961	1.47	0.813	0.801	0.801	0.523
MS-Random	0.409	2.64	0.544	0.554	0.439	0.967	1.27	0.821	0.816	0.822	0.537
ATC-NE	0.530	3.80	0.506	0.642	0.408	0.849	3.59	0.684	0.706	0.749	0.670
ATC-MC	0.528	3.76	0.507	0.642	0.406	0.863	3.54	0.698	0.716	0.749	0.671

(b) Results on sentiment analysis (SA) datasets.

Measure	CNN					RoBERTa					
	R^2	MAE	Macro τ	Micro τ	ID τ	R^2	MAE	Macro τ	Micro τ	ID τ	Arch τ
MS-SSMBA	0.575	2.09	0.570	0.534	0.704	0.933	1.19	0.750	0.730	0.771	0.301
MS-EDA	0.577	2.04	0.581	0.511	0.709	0.941	1.26	0.789	0.757	0.799	0.572
MS-BT	0.509	2.11	0.470	0.449	0.584	0.944	1.07	0.759	0.740	0.778	0.563
MS-Random	0.451	2.20	0.452	0.428	0.570	0.890	1.70	0.688	0.647	0.710	0.401
ATC-NE	0.378	3.57	0.430	0.294	0.705	0.673	2.35	0.536	0.520	0.749	0.442
ATC-MC	0.382	3.57	0.433	0.297	0.706	0.718	2.21	0.570	0.556	0.750	0.445

(c) Results on natural language inference (NLI) datasets

Table 2: Evaluation metrics measuring the correlation of our smoothness measure with OOD generalization. The best performing measures for each metric are bolded. On all tasks, our smoothness measure achieves strong generalization and beats baseline methods in almost all metrics.

We also compare our method against output based methods that directly predict OOD generalization. We use **ATC-MC** and **ATC-NE** [19] as our two baselines, which calculate a threshold on validation data based on max confidence and negative entropy scores respectively. To calculate τ metrics on these methods we treat the generated accuracy predictions as a score, and for R^2 and MAE we use the accuracy predictions directly. To calculate ID τ values we select a threshold value based on validation data then calculate predicted accuracy values on test data from the same domain.

5 Results

5.1 Correlation with OOD Generalization

We first present results analyzing the correlation of our proposed manifold smoothness measure with OOD generalization in Table 2. We report R^2 , MAE, Macro τ , Micro τ , ID τ , and Arch τ as detailed in Section 3.3. We omit results on Spectral and Frobenius norm measures as they are close to 0 or negative for all metrics.

Image Classification Results on image classification tasks are presented in Table 2a. Our smoothness measure based on RandAugment significantly outperforms ATC based methods and all other measures on all metrics. MS-RandAug also exhibits only a small decrease in correlation when moving from in-domain to OOD datasets, compared to ATC methods which suffer a much larger drop. Interestingly, patch erasing and flip and crops fail to achieve strong correlations, indicating that they may poorly reflect the true image manifold.

Measure	CNN		RoBERTa	
	R^2	Micro τ	R^2	Micro τ
MS-SSMBA	0.584	0.566	0.941	0.816
MS-EDA	0.575	0.567	0.884	0.715
MS-BT	0.538	0.470	0.906	0.766
MS-Random	0.277	0.373	0.918	0.776
ATC-NE	0.271	0.495	0.329	0.356
ATC-MC	0.295	0.506	0.437	0.436

(a) Results on the Drugs . com dataset.

Measure	CNN		RoBERTa	
	R^2	Micro τ	R^2	Micro τ
MS-SSMBA	0.083	0.080	0.691	0.463
MS-EDA	0.202	0.110	0.739	0.540
MS-BT	0.213	0.247	0.730	0.527
MS-Random	0.096	0.102	0.030	0.012
ATC-NE	0.077	-0.107	0.719	0.345
ATC-MC	0.076	-0.106	0.734	0.354

(b) Results on the MedNLI dataset.

Table 3: Evaluation metrics measuring the correlation of our smoothness measure with generalization on extreme OOD datasets. MS-* methods beat baselines on both tasks, with RoBERTa models exhibiting only a slight degradation in correlation compared to more typical OOD settings.

Sentiment Analysis (SA) Results on Sentiment Analysis tasks are presented in Table 2b. In experiments on both architectures, our smoothness measures achieves strong correlation with OOD generalization on all metrics and beat all baselines. Of the neighborhoods tested, MS-SSMBA performs the best across both architectures. On cross architecture analysis, we observe strong Arch τ for our neighborhood measures, although they are outperformed by both ATC methods. We observe particularly strong correlation on RoBERTa models, with a nearly perfectly linear R^2 value of 0.972 and large Micro τ of 0.829. We hypothesize that this is due to the pretrained initialization of RoBERTa models, which gives a strong inductive bias towards learning a space aligned with the one in which we measure smoothness. In contrast, CNN models are trained from random initializations and may not learn as closely aligned a space.

Natural Language Inference (NLI) Results on Natural Language Inference tasks are presented in Table 2c. Similar to our sentiment analysis results, our manifold smoothness measures achieve strong correlation with OOD generalization on both architectures and beat all baselines. Correlations in general on NLI are lower than those of sentiment analysis, perhaps because the sentence pair data manifold is more complex and difficult to learn compared to the single sentence data manifold. This also explains why we observe no single best performing neighborhood, as defining the distribution $q(x'|x)$ for sentence pairs is much more difficult. As in sentiment analysis experiments we observe exceptionally high correlation on RoBERTa models, for which we offer a similar hypothesis as above. On cross architecture analysis, we again observe strong correlation for our smoothness measures that outperform both ATC methods.

5.2 Extreme OOD Generalization

We now consider more extreme generalization to data domains with specialized and knowledge intensive data. We consider only natural language tasks as it is difficult to find a sufficiently specialized image classification dataset that maintains the same output classes. For sentiment analysis we use the Drugs . com review dataset [23], and for natural language inference we use MedNLI [62], an NLI dataset generated from clinical notes and patient history. Both these datasets contain sentences with highly specific medical terms and phrases not seen in any of our training domains. All models from all original training domains are evaluated on each of these extreme OOD domains, and we report R^2 and Micro τ . Results are shown in Table 3

On the Drugs . com dataset, we observe only a small decrease in correlation for both model architectures. However, ATC methods begin to fail here, with Micro τ on RoBERTa models dropping significantly from 0.706 to 0.356. This suggests that models become poorly calibrated in extreme OOD settings, making output based OOD prediction methods more fragile.

On MedNLI we observe a much larger drop in correlation for both model types. For CNN models, most of our measures fail to correlate at all, and ATC methods degrade so much they became anti correlated with generalization. For RoBERTa models we observe only minor drops in correlation for all measures. Surprisingly, ATC R^2 values actually increase compared to our original experiments, although Micro τ decreases. For both tasks MS-Random exhibits almost no correlation with OOD generalization. This suggests that the choice of neighborhood becomes much more important as we move farther from our training domain.

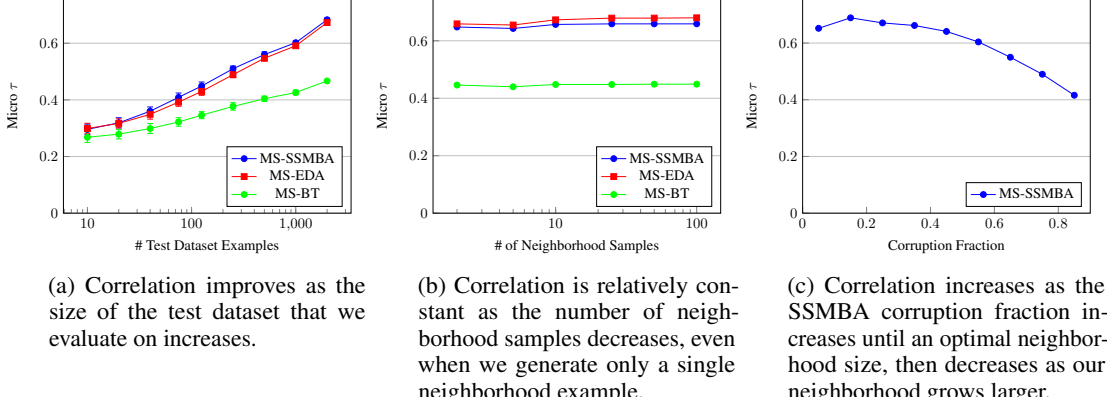


Figure 3: Micro τ for our smoothness measure calculated with varying ablations on CNN models evaluated on Amazon toy reviews.

5.3 Smoothness Estimation Ablations

In this section we examine factors that may affect the quality of the smoothness estimation generated from our measure. Since rerunning all of our experiments is too costly, we focus on evaluating CNN models trained on the sentiment analysis task. Specifically, we evaluate only on Amazon reviews of toys using a pool of CNN models trained on all other domains.

Test Dataset Size Does our manifold smoothness measure still correlate well when the test dataset is small? We randomly and iteratively subsample our test dataset of 2000 examples to reduce our dataset size down to 10 examples. We then measure our models’ smoothness on each subsampled dataset and calculate the Micro τ on all models. Results are shown in Figure 3a. We find that for all neighborhoods, smaller datasets lead to noisier smoothness estimates and lower correlation. As dataset size increases, correlation increases as well.

Number of Samples Generated How many examples do we need to sample from our neighborhood in order to generate a reliable smoothness estimate? We generate a varying number of samples for each test example, from a minimum of a single example to a maximum of 100 examples. We then estimate our smoothness measure with each set of neighborhood samples and calculate the micro τ as before. Results are shown in Figure 3b. We find that our measure is surprisingly robust to the number of neighborhood samples, with only a small difference between 100 samples and a single sample. For all measures, correlation slightly increases as the number of samples increases and we achieve a better estimation of the true smoothness value.

Neighborhood Size Does the quality of our measure depend on how large of a neighborhood we sample from? We define the neighborhood size as the level of noise in our neighborhood distribution $q(x'|x)$, since a noisier distribution will generate points farther from x . For our experiments we use MS-SSMBA and vary the corruption percentage from a minimum of 5% to a maximum of 85%. After generating sets of neighborhood examples from each distribution, we estimate our models’ smoothness on each one and calculate the micro τ on all models. Results are shown in Figure 3c. We find that as we begin to increase the neighborhood size, correlation begins to increase as well. Correlation quickly reaches a maximum, then decreases as we continue to increase our neighborhood size. However, even at a 85% corruption, our method is quite robust and achieves a micro τ of 0.416.

6 Discussion

In this paper, motivated by the limited settings in which existing complexity measures can be applied, we develop a *local manifold smoothness* measure that can be applied even when test distributions are unknown and model training data, weights, and gradients are unavailable. We evaluate our method on image classification, sentiment analysis, and natural language inference datasets, calculating a variety of correlation metrics on both in-domain and out-of-domain test sets. Across all tasks and experimental settings, we find that our smoothness measure outperforms baseline methods in all metrics except one. However, our method has several limitations. We cannot compare against

other complexity measures since they can't be applied in our OOD experimental settings. Local manifold smoothness also depends on access to a neighborhood distribution $q(x'|x)$ from which we can sample. In settings where $q(x'|x)$ is difficult to define, the applicability of our method may vary so practitioners must be careful to verify their estimates on a labelled test set. In future work we plan to apply smoothness as a method for OOD detection.

References

- [1] S. Aithal K, D. Kashyap, and N. Subramanyam. Robustness to Augmentations as a Generalization metric. *arXiv e-prints*, art. arXiv:2101.06459, Jan. 2021.
- [2] Z. Allen-Zhu, Y. Li, and Y. Liang. Learning and Generalization in Overparameterized Neural Networks, Going Beyond Two Layers. *arXiv e-prints*, art. arXiv:1811.04918, Nov. 2018.
- [3] M. Arbel, D. J. Sutherland, M. a. Bińkowski, and A. Gretton. On gradient regularizers for mmd gans. In S. Bengio, H. Wallach, H. Larochelle, K. Grauman, N. Cesa-Bianchi, and R. Garnett, editors, *Advances in Neural Information Processing Systems*, volume 31. Curran Associates, Inc., 2018. URL <https://proceedings.neurips.cc/paper/2018/file/07f75d9144912970de5a09f5a305e10c-Paper.pdf>.
- [4] M. Arjovsky, L. Bottou, I. Gulrajani, and D. Lopez-Paz. Invariant risk minimization. *arXiv*, 2019.
- [5] P. L. Bartlett and S. Mendelson. Rademacher and gaussian complexities: Risk bounds and structural results. *J. Mach. Learn. Res.*, 3(null):463–482, mar 2003. ISSN 1532-4435.
- [6] P. L. Bartlett, D. J. Foster, and M. J. Telgarsky. Spectrally-normalized margin bounds for neural networks. In I. Guyon, U. V. Luxburg, S. Bengio, H. Wallach, R. Fergus, S. Vishwanathan, and R. Garnett, editors, *Advances in Neural Information Processing Systems*, volume 30. Curran Associates, Inc., 2017. URL <https://proceedings.neurips.cc/paper/2017/file/b22b257ad0519d4500539da3c8bcf4dd-Paper.pdf>.
- [7] S. Ben-David, J. Blitzer, K. Crammer, and F. Pereira. Analysis of representations for domain adaptation. In B. Schölkopf, J. Platt, and T. Hoffman, editors, *Advances in Neural Information Processing Systems*, volume 19. MIT Press, 2007. URL <https://proceedings.neurips.cc/paper/2006/file/b1b0432ceafb0ce714426e9114852ac7-Paper.pdf>.
- [8] O. Chapelle, B. Schölkopf, and A. Zien. *Semi-Supervised Learning (Adaptive Computation and Machine Learning)*. The MIT Press, 2006. ISBN 0262033585.
- [9] M. Chen*, K. Goel*, N. Sohoni*, F. Poms, K. Fatahalian, and C. Re. Mandoline: Model evaluation under distribution shift. *International Conference of Machine Learning (ICML)*, 2021.
- [10] C.-Y. Chuang, A. Torralba, and S. Jegelka. Estimating generalization under distribution shifts via domain-invariant representations. *International conference on machine learning*, 2020.
- [11] E. D. Cubuk, B. Zoph, J. Shlens, and Q. Le. Randaugment: Practical automated data augmentation with a reduced search space. In H. Larochelle, M. Ranzato, R. Hadsell, M. Balcan, and H. Lin, editors, *Advances in Neural Information Processing Systems*, volume 33, pages 18613–18624. Curran Associates, Inc., 2020. URL <https://proceedings.neurips.cc/paper/2020/file/d85b63ef0ccb114d0a3bb7b7d808028f-Paper.pdf>.
- [12] L. N. Darlow, E. J. Crowley, A. Antoniou, and A. J. Storkey. CINIC-10 is not ImageNet or CIFAR-10. *arXiv e-prints*, art. arXiv:1810.03505, Oct. 2018.
- [13] L. Deng. The mnist database of handwritten digit images for machine learning research. *IEEE Signal Processing Magazine*, 29(6):141–142, 2012.
- [14] W. Deng and L. Zheng. Are labels always necessary for classifier accuracy evaluation? In *Proc. CVPR*, 2021.
- [15] W. Deng, S. Gould, and L. Zheng. What does rotation prediction tell us about classifier accuracy under varying testing environments? In *ICML*, 2021.
- [16] G. K. Dziugaite and D. M. Roy. Computing nonvacuous generalization bounds for deep (stochastic) neural networks with many more parameters than training data. In *Proceedings of the 33rd Annual Conference on Uncertainty in Artificial Intelligence (UAI)*, 2017.

[17] G. Elsayed, D. Krishnan, H. Mobahi, K. Regan, and S. Bengio. Large margin deep networks for classification. In S. Bengio, H. Wallach, H. Larochelle, K. Grauman, N. Cesa-Bianchi, and R. Garnett, editors, *Advances in Neural Information Processing Systems*, volume 31. Curran Associates, Inc., 2018. URL <https://proceedings.neurips.cc/paper/2018/file/42998cf32d552343bc8e460416382dca-Paper.pdf>.

[18] P. Foret, A. Kleiner, H. Mobahi, and B. Neyshabur. Sharpness-Aware Minimization for Efficiently Improving Generalization. *art. arXiv:2010.01412*, 2020.

[19] S. Garg, S. Balakrishnan, Z. C. Lipton, B. Neyshabur, and H. Sedghi. Leveraging Unlabeled Data to Predict Out-of-Distribution Performance. *arXiv e-prints*, art. arXiv:2201.04234, Jan. 2022.

[20] V. Garg, A. Tauman Kalai, K. Ligett, and S. Wu. Learn to expect the unexpected: Probably approximately correct domain generalization. In A. Banerjee and K. Fukumizu, editors, *Proceedings of The 24th International Conference on Artificial Intelligence and Statistics*, volume 130 of *Proceedings of Machine Learning Research*, pages 3574–3582. PMLR, 13–15 Apr 2021. URL <https://proceedings.mlr.press/v130/garg21a.html>.

[21] S. A. Glantz, B. K. Slinker, and T. B. Neilands. *Primer of Applied Regression and Analysis of Variance*. Health Professions Division, McGraw-Hill, New York, 1990.

[22] I. Goodfellow, J. Shlens, and C. Szegedy. Explaining and harnessing adversarial examples. *arXiv 1412.6572*, 12 2014.

[23] F. Gräßer, S. Kallumadi, H. Malberg, and S. Zaunseder. Aspect-based sentiment analysis of drug reviews applying cross-domain and cross-data learning. In *Proceedings of the 2018 International Conference on Digital Health*, DH ’18, page 121–125, New York, NY, USA, 2018. Association for Computing Machinery. ISBN 9781450364935. doi: 10.1145/3194658.3194677. URL <https://doi.org/10.1145/3194658.3194677>.

[24] D. Guillory, V. Shankar, S. Ebrahimi, T. Darrell, and L. Schmidt. Predicting with Confidence on Unseen Distributions. In *International Conference on Computer Vision*, 2021.

[25] I. Gulrajani, F. Ahmed, M. Arjovsky, V. Dumoulin, and A. Courville. Improved training of wasserstein gans. In *Proceedings of the 31st International Conference on Neural Information Processing Systems*, NIPS’17, page 5769–5779, Red Hook, NY, USA, 2017. Curran Associates Inc. ISBN 9781510860964.

[26] A. Gupta, A. Anpalagan, L. Guan, and A. S. Khwaja. Deep learning for object detection and scene perception in self-driving cars: Survey, challenges, and open issues. *Array*, 10: 100057, 2021. ISSN 2590-0056. doi: <https://doi.org/10.1016/j.array.2021.100057>. URL <https://www.sciencedirect.com/science/article/pii/S2590005621000059>.

[27] D. Hendrycks, X. Liu, E. Wallace, A. Dziedzic, R. Krishnan, and D. Song. Pretrained transformers improve out-of-distribution robustness. In *Proceedings of the 58th Annual Meeting of the Association for Computational Linguistics*, pages 2744–2751, Online, July 2020. Association for Computational Linguistics. doi: 10.18653/v1/2020.acl-main.244. URL <https://aclanthology.org/2020.acl-main.244>.

[28] D. Hendrycks, X. Liu, E. Wallace, A. Dziedzic, R. Krishnan, and D. Song. Pretrained transformers improve out-of-distribution robustness. In *Association for Computational Linguistics*, 2020.

[29] Y. Jiang, D. Krishnan, H. Mobahi, and S. Bengio. Predicting the generalization gap in deep networks with margin distributions. In *Proceedings of ICLR*, 2018.

[30] Y. Jiang, B. Neyshabur, H. Mobahi, D. Krishnan, and S. Bengio. Fantastic Generalization Measures and Where to Find Them. *arXiv e-prints*, art. arXiv:1912.02178, Dec. 2019.

[31] Y. Jiang, P. Foret, S. Yak, D. M. Roy, H. Mobahi, G. Karolina Dziugaite, S. Bengio, S. Gunasekar, I. Guyon, and B. Neyshabur. NeurIPS 2020 Competition: Predicting Generalization in Deep Learning. *arXiv e-prints*, art. arXiv:2012.07976, Dec. 2020.

[32] Y. Jiang, V. Nagarajan, C. Baek, and J. Zico Kolter. Assessing Generalization of SGD via Disagreement. *arXiv e-prints*, art. arXiv:2106.13799, June 2021.

[33] M. G. Kendall. A new measure of rank correlation. *Biometrika*, 30(1/2):81–93, 1938. ISSN 00063444. URL <http://www.jstor.org/stable/2332226>.

[34] N. S. Keskar, D. Mudigere, J. Nocedal, M. Smelyanskiy, and P. T. P. Tang. On large-batch training for deep learning: Generalization gap and sharp minima. *arXiv preprint arXiv:1609.04836*, 2016.

[35] Y. Kim. Convolutional neural networks for sentence classification. In *Proceedings of the 2014 Conference on Empirical Methods in Natural Language Processing (EMNLP)*, 2014.

[36] D. P. Kingma and J. Ba. Adam: A method for stochastic optimization, 2014. URL <http://arxiv.org/abs/1412.6980>. cite arxiv:1412.6980Comment: Published as a conference paper at the 3rd International Conference for Learning Representations, San Diego, 2015.

[37] P. W. Koh, S. Sagawa, H. Marklund, S. M. Xie, M. Zhang, A. Balsubramani, W. Hu, M. Yasunaga, R. L. Phillips, I. Gao, T. Lee, E. David, I. Stavness, W. Guo, B. A. Earnshaw, I. S. Haque, S. Beery, J. Leskovec, A. Kundaje, E. Pierson, S. Levine, C. Finn, and P. Liang. WILDS: A benchmark of in-the-wild distribution shifts. In *International Conference on Machine Learning (ICML)*, 2021.

[38] A. Krizhevsky. Learning multiple layers of features from tiny images. Technical report, 2009.

[39] T. Liang, T. Poggio, A. Rakhlin, and J. Stokes. Fisher-rao metric, geometry, and complexity of neural networks. In K. Chaudhuri and M. Sugiyama, editors, *Proceedings of the Twenty-Second International Conference on Artificial Intelligence and Statistics*, volume 89 of *Proceedings of Machine Learning Research*, pages 888–896. PMLR, 16–18 Apr 2019. URL <https://proceedings.mlr.press/v89/liang19a.html>.

[40] W. Liang and J. Zou. Metashift: A dataset of datasets for evaluating contextual distribution shifts and training conflicts. In *International Conference on Learning Representations*, 2022. URL <https://openreview.net/forum?id=MTex8qKavoS>.

[41] M. Lin, Q. Chen, and S. Yan. Network In Network. *arXiv e-prints*, art. arXiv:1312.4400, Dec. 2013.

[42] Y. Liu, M. Ott, N. Goyal, J. Du, M. Joshi, D. Chen, O. Levy, M. Lewis, L. Zettlemoyer, and V. Stoyanov. Roberta: A robustly optimized bert pretraining approach. *arXiv preprint arXiv:1907.11692*, 2019.

[43] S. Lu, B. Nott, A. Olson, A. Todeschini, H. Vahabi, Y. Carmon, and L. Schmidt. Harder or different? a closer look at distribution shift in dataset reproduction. In *ICML Workshop on Uncertainty and Robustness in Deep Learning*, 2020.

[44] D. A. McAllester. Pac-bayesian model averaging. In *Proceedings of the Twelfth Annual Conference on Computational Learning Theory*, COLT '99, page 164–170, New York, NY, USA, 1999. Association for Computing Machinery. ISBN 1581131674. doi: 10.1145/307400.307435. URL <https://doi.org/10.1145/307400.307435>.

[45] T. Miyato, T. Kataoka, M. Koyama, and Y. Yoshida. Spectral normalization for generative adversarial networks. In *International Conference on Learning Representations*, 2018.

[46] L. Mou, R. Men, G. Li, Y. Xu, L. Zhang, R. Yan, and Z. Jin. Natural language inference by tree-based convolution and heuristic matching. In *Proceedings of the 54th Annual Meeting of the Association for Computational Linguistics (Volume 2: Short Papers)*, pages 130–136, Berlin, Germany, Aug. 2016. Association for Computational Linguistics. doi: 10.18653/v1/P16-2022. URL <https://aclanthology.org/P16-2022>.

[47] V. Nagarajan and J. Z. Kolter. Generalization in deep networks: The role of distance from initialization. In *NeurIPS Workshop on Deep Learning: Bridging Theory and Practice*, 2019.

[48] Y. Netzer, T. Wang, A. Coates, A. Bissacco, B. Wu, and A. Ng. Reading digits in natural images with unsupervised feature learning. In *NIPS Workshop on Deep Learning and Unsupervised Feature Learning*, 2011.

[49] B. Neyshabur, R. R. Salakhutdinov, and N. Srebro. Path-sgd: Path-normalized optimization in deep neural networks. In C. Cortes, N. Lawrence, D. Lee, M. Sugiyama, and R. Garnett, editors, *Advances in Neural Information Processing Systems*, volume 28. Curran Associates, Inc., 2015. URL <https://proceedings.neurips.cc/paper/2015/file/eaa32c96f620053cf442ad32258076b9-Paper.pdf>.

[50] B. Neyshabur, R. Tomioka, and N. Srebro. Norm-based capacity control in neural networks. In P. Grünwald, E. Hazan, and S. Kale, editors, *Proceedings of The 28th Conference on Learning Theory*, volume 40 of *Proceedings of Machine Learning Research*, pages 1376–1401, Paris, France, 03–06 Jul 2015. PMLR. URL <https://proceedings.mlr.press/v40/Neyshabur15.html>.

[51] B. Neyshabur, S. Bhojanapalli, D. McAllester, and N. Srebro. Exploring generalization in deep learning. In *Proceeding of NeurIPS*, 2017.

[52] B. Neyshabur, S. Bhojanapalli, and N. Srebro. A pac-bayesian approach to spectrally-normalized margin bounds for neural networks. In *International Conference on Learning Representations*, 2017.

[53] N. Ng, K. Yee, A. Baevski, M. Ott, M. Auli, and S. Edunov. Facebook FAIR’s WMT19 news translation task submission. In *Proceedings of the Fourth Conference on Machine Translation (Volume 2: Shared Task Papers, Day 1)*, pages 314–319, Florence, Italy, Aug. 2019. Association for Computational Linguistics. doi: 10.18653/v1/W19-5333. URL <https://aclanthology.org/W19-5333>.

[54] N. Ng, K. Cho, and M. Ghassemi. Ssmba: Self-supervised manifold based data augmentation for improving out-of-domain robustness. In *Proc. of EMNLP*, 2020.

[55] J. Ni, J. Li, and J. McAuley. Justifying recommendations using distantly-labeled reviews and fine-grained aspects. In *Proceedings of EMNLP*, 2019.

[56] M. Ott, S. Edunov, A. Baevski, A. Fan, S. Gross, N. Ng, D. Grangier, and M. Auli. fairseq: A fast, extensible toolkit for sequence modeling. In *Proceedings of NAACL-HLT 2019: Demonstrations*, 2019.

[57] N. Papernot, P. McDaniel, I. Goodfellow, S. Jha, Z. B. Celik, and A. Swami. Practical black-box attacks against machine learning. In *Proceedings of the 2017 ACM on Asia Conference on Computer and Communications Security*, ASIA CCS ’17, page 506–519, New York, NY, USA, 2017. Association for Computing Machinery. ISBN 9781450349444. doi: 10.1145/3052973.3053009. URL <https://doi.org/10.1145/3052973.3053009>.

[58] G. Pereyra, G. Tucker, J. Chorowski, Ł. Kaiser, and G. Hinton. Regularizing neural networks by penalizing confident output distributions. In *ICLR*, 2017.

[59] B. Recht, R. Roelofs, L. Schmidt, and V. Shankar. Do cifar-10 classifiers generalize to cifar-10? 2018. <https://arxiv.org/abs/1806.00451>.

[60] B. Recht, R. Roelofs, L. Schmidt, and V. Shankar. Do ImageNet classifiers generalize to ImageNet? In K. Chaudhuri and R. Salakhutdinov, editors, *Proceedings of the 36th International Conference on Machine Learning*, volume 97 of *Proceedings of Machine Learning Research*, pages 5389–5400. PMLR, 09–15 Jun 2019. URL <https://proceedings.mlr.press/v97/recht19a.html>.

[61] A. B. Rico Sennrich, Barry Haddow. Improving neural machine translation models with monolingual data. In *Proc. of ACL*, 2016.

[62] A. Romanov and C. Shivade. Lessons from natural language inference in the clinical domain. URL <http://arxiv.org/abs/1808.06752>.

[63] M. Rosca, T. Weber, A. Gretton, and S. Mohamed. A case for new neural network smoothness constraints. In *NeurIPS ICBINB Workshop*, 2020.

[64] Y. Schiff, B. Quanz, P. Das, and P.-Y. Chen. Predicting deep neural network generalization with perturbation response curves. In *Neural Information Processing Systems*, 2021.

[65] K. Simonyan and A. Zisserman. Very deep convolutional networks for large-scale image recognition. In *Proceedings of the International Conference on Learning Representations*, 2015.

[66] R. Taori, A. Dave, V. Shankar, N. Carlini, B. Recht, and L. Schmidt. Measuring robustness to natural distribution shifts in image classification. In H. Larochelle, M. Ranzato, R. Hadsell, M. Balcan, and H. Lin, editors, *Advances in Neural Information Processing Systems*, volume 33, pages 18583–18599. Curran Associates, Inc., 2020. URL <https://proceedings.neurips.cc/paper/2020/file/d8330f857a17c53d217014ee776bfd50-Paper.pdf>.

[67] V. N. Vapnik and A. Y. Chervonenkis. On the uniform convergence of relative frequencies of events to their probabilities. *Theory of Probability & Its Applications*, 16(2):264–280, 1971. doi: 10.1137/1116025. URL <https://doi.org/10.1137/1116025>.

[68] R. Vedantam, D. Lopez-Paz, and D. J. Schwab. An empirical investigation of domain generalization with empirical risk minimizers. In *Neural Information Processing Systems*, 2021.

[69] J. Wei and K. Zou. EDA: Easy data augmentation techniques for boosting performance on text classification tasks. In *Proceedings of the 2019 Conference on Empirical Methods in Natural Language Processing and the 9th International Joint Conference on Natural Language Processing (EMNLP-IJCNLP)*, pages 6383–6389, Hong Kong, China, Nov. 2019. Association for Computational Linguistics. URL <https://www.aclweb.org/anthology/D19-1670>.

[70] J. Wiens, S. Saria, M. Sendak, M. Ghassemi, V. Liu, F. Doshi-Velez, K. Jung, K. Heller, D. Kale, M. Saeed, P. Ossorio, S. Thadaney-Israni, and A. Goldenberg. Do no harm: A roadmap for responsible machine learning for healthcare. *Nature Medicine*, 25(10):1337–1340, 2019.

[71] A. Williams, N. Nangia, and S. Bowman. A broad-coverage challenge corpus for sentence understanding through inference. In *Proceedings of the 2018 Conference of the North American Chapter of the Association for Computational Linguistics: Human Language Technologies, Volume 1 (Long Papers)*, pages 1112–1122. Association for Computational Linguistics, 2018. URL <http://aclweb.org/anthology/N18-1101>.

[72] L. Xie, J. Wang, Z. Wei, M. Wang, and Q. Tian. DisturbLabel: Regularizing CNN on the Loss Layer. *arXiv e-prints*, art. arXiv:1605.00055, Apr. 2016.

[73] Q. Xie, Z. Dai, E. Hovy, M.-T. Luong, and Q. V. Le. Unsupervised data augmentation for consistency training. *arXiv preprint arXiv:1904.12848*, 2019.

[74] Y. Yoshida and T. Miyato. Spectral Norm Regularization for Improving the Generalizability of Deep Learning. *arXiv e-prints*, art. arXiv:1705.10941, May 2017.

[75] C. Zhang, S. Bengio, M. Hardt, B. Recht, and O. Vinyals. Understanding deep learning requires rethinking generalization. *arXiv e-prints*, art. arXiv:1611.03530, Nov. 2016.

[76] Y. Zhang, T. Liu, M. Long, and M. Jordan. Bridging theory and algorithm for domain adaptation. In K. Chaudhuri and R. Salakhutdinov, editors, *Proceedings of the 36th International Conference on Machine Learning*, volume 97 of *Proceedings of Machine Learning Research*, pages 7404–7413. PMLR, 09–15 Jun 2019. URL <https://proceedings.mlr.press/v97/zhang19i.html>.

[77] Z. Zhong, L. Zheng, G. Kang, S. Li, and Y. Yang. Random erasing data augmentation. *Proceedings of the AAAI Conference on Artificial Intelligence*, 34(07):13001–13008, Apr. 2020. doi: 10.1609/aaai.v34i07.7000. URL <https://ojs.aaai.org/index.php/AAAI/article/view/7000>.

Hyperparameter	CNN		RoBERTa	
	SA	NLI	SA	NLI
Batch Size	{32, 64, 128}	{32, 64, 128 }	{8, 16, 32}	{8, 16, 32}
Depth	{1, 2, 3 }	{1, 2, 3 }	1	1
Width	{128, 256, 512}	{128, 256, 512 }	768	768
Dropout	{0.0, 0.25}	{0.0, 0.25}	{0.0, 0.1}	{0.0, 0.1}
Weight Decay	{0.0, 0.0001, 0.0005}	0.0	{0.0, 0.0001, 0.0005}	{0.0, 0.0001, 0.0005}
Label Noise	0.0	{0.0, 0.2, 0.4}	{0.0, 0.2, 0.4}	{0.0, 0.2, 0.4}

Table 4: Possible hyperparameter values for each architecture and task.

A Experimental Setup

In this section we present full details of our experimental setup, including data preprocessing and specifics on model architecture and hyperparameter space. All models are trained on a single RTX6000 GPU.

A.1 Data Preprocessing

Image classification datasets are preprocessed by normalizing pixel values and resizing to 32×32 if necessary. We use the same preprocessing steps for sentiment analysis and NLI experiments. All data is first tokenized using a GPT-2 style tokenizer and BPE vocabulary provided by `fairseq` [56]. This BPE vocabulary consists of 50263 types. Corresponding labels are encoded using a label dictionary consisting of as many types as there are classes. Input text and labels are then binarized for model training.

A.2 Model Architecture

Our image classification models are Network in Network (NiN) [41], VGG [65], and CNN models. Training and hyperparameter details for these models are provided in Jiang et al. [31].

Our CNN models are based on the architecture in [35]. Our input embeddings are 512 dimensional, which we treat as our channel dimension. Our base model applies a set of three one dimensional convolutions of kernel size 3, 4, and 5 with 256 output channels. We modulate the number of stacked convolutions (depth) as well as the channel size (width). Each convolution generates a separate representation that is max pooled across the sequence and concatenated together. We feed this representation into a MLP classifier with a single hidden layer of 512 dimensions. We apply dropout of 0.2 to our inputs and MLP classifier.

Our RoBERTa models use a pre-trained RoBERTa_{BASE} model provided by `fairseq`. Classification token embeddings are fed into an MLP classifier with a single hidden layer of 512 dimensions. All models are written within the `fairseq` framework [56] and trained on a single RTX6000 or T4 GPU.

A.3 Model Hyperparameters

Hyperparameter values for image classification models are provided in Jiang et al. [31]. For natural language models we vary the following hyperparameters: training domain, batch size, depth, width, dropout, weight decay, and label noise. For training domains on sentiment analysis we choose between `books`, `clothing`, `home`, `kindle`, `movies`, `pets`, `sports`, `tech`, `tools`, `toys`. For training domains on NLI, we choose between `slate`, `government`, `fiction`, `telephone`, `travel`. NLI datasets include additional test sets `oup`, `nineeleven`, `facetoface`, `verbatim`, `letters`. Possible values for all other hyperparameters are provided in Table 4

A.4 Model Training

All models are trained with the Adam optimizer [36] with $\beta = (0.9, 0.98)$ and $\epsilon = 1 \times 10^{-6}$. CNN models are trained with learning rate 1×10^{-3} and RoBERTa models are trained with learning rate 1×10^{-5} . We use a inverse square root learning rate scheduler to anneal learning rate over training. We early stop CNN models on sentiment analysis at 0.04 cross entropy and on NLI at 0.03 cross

entropy. We early stop RoBERTa models on sentiment analysis at 0.05 cross entropy and on NLI at 0.3 cross entropy. Training details for image classification models are provided in Jiang et al. [31].

A.5 Neighborhood Hyperparameters

We select hyperparameters for our neighborhood distributions based on best practices provided in their respective papers. For RandAugment we use a magnitude parameter of 15 and augment only once. For FlipCrop we flip the image horizontally with probability 50% and generate a crop with a lower bound of 8% of total image area and an aspect ratio between 3/4 and 4/3. Images are resized to 32×32 after cropping. For Erase we select a region to erase with a maximum size of 33% of the total image area and an aspect ratio between 1/3 and 10/3.

For SSMBA, we select 15% of tokens to corrupt, leaving 10% of them unmasked, randomly replacing 10% of them, and masking the remaining 80%. We reconstruct these corrupted sentences with a RoBERTa base model [42]. For EDA, we apply all operations on 10% of tokens. For backtranslation, we use English to German and German to English models provided in [53]. For our random baseline, we randomly replace 15% of tokens.

B Additional Experiments

B.1 Norm-Based Complexity Measures

Following [30], we calculate our spectral norm measure as $\Pi_{i=1}^d \|\mathbf{W}_i\|_2^2$ and Frobenius norm measure $\Pi_{i=1}^d \|\mathbf{W}_i\|_F^2$. We do not list results on these measures as the correlations are often negative or 0.

B.2 Cross-Domain Correlation

In this set of experiments we measure the correlation between smoothness and generalization values of a single model trained on a single training domain evaluated across different OOD test domains. We call these the **CNN** τ and **Roberta** τ when averaged respectively across CNN and RoBERTa models and training domains. Results are presented in Table 5.

For both models and both tasks, our smoothness measure performs quite poorly, although they still outperform ATC baselines. We hypothesize that different regions of the input space have different optimal levels of smoothness that achieve the lowest generalization error. Our value of interest is then not the absolute smoothness, but the *relative* smoothness compared to this optimal value. These values are the same when comparing different models evaluated on the same domain, but are not the same for the same model evaluated on different domains, making correlating across domains difficult. We note that MS-Random achieves the best correlation for almost all experiments, a phenomenon we plan to investigate in future work.

B.3 Negative Entropy Results

A full table of results including metrics calculated on smoothness measured with negative entropy is provided in Table 6. We refer to measures calculated with entropy as **MSE-SSMBA**, **MSE-EDA**, **MSE-BT**, and **MSE-Random**. For most metrics, MSE-* methods perform similarly or slightly worse.

Task	Measure	CNN τ	RoBERTa τ
SA	MS-SSMBA	0.360	0.010
	MS-EDA	0.431	0.266
	MS-BT	0.505	0.245
	MS-Random	0.570	0.150
	ATC-NE	0.543	0.228
	ATC-MC	0.539	0.224
NLI	MS-SSMBA	0.022	0.260
	MS-EDA	0.102	0.335
	MS-BT	0.089	0.333
	MS-Random	0.226	0.440
	ATC-NE	0.219	0.231
	ATC-MC	0.223	0.239

Table 5: Correlation metrics evaluating the ability of our smoothness measure to predict OOD generalization across test datasets. Our smoothness measures fail in these cases and underperform baselines.

Task	Measure	CNN				RoBERTa			
		R^2	MAE	Macro τ	Micro τ	R^2	MAE	Macro τ	Micro τ
SA	MS-SSMBA	0.662	1.93	0.677	0.689	0.972	1.29	0.832	0.829
	MS-EDA	0.641	2.04	0.664	0.649	0.968	1.45	0.830	0.810
	MS-BT	0.550	2.99	0.592	0.501	0.961	1.47	0.813	0.801
	MS-Random	0.409	2.64	0.544	0.554	0.967	1.27	0.821	0.816
	MSE-SSMBA	0.595	2.53	0.708	0.713	0.971	1.32	0.830	0.824
	MSE-EDA	0.534	2.71	0.698	0.674	0.965	1.55	0.825	0.801
	MSE-BT	0.471	3.59	0.618	0.541	0.961	1.46	0.813	0.799
	MSE-Random	0.283	3.37	0.570	0.552	0.964	1.34	0.818	0.809
	ATC-NE	0.530	3.80	0.506	0.642	0.849	3.59	0.684	0.706
	ATC-MC	0.528	3.76	0.507	0.642	0.863	3.54	0.698	0.716
NLI	MS-SSMBA	0.575	2.09	0.570	0.534	0.933	1.19	0.750	0.730
	MS-EDA	0.577	2.04	0.581	0.511	0.941	1.26	0.789	0.757
	MS-BT	0.509	2.11	0.470	0.449	0.944	1.07	0.759	0.740
	MS-Random	0.451	2.20	0.452	0.428	0.890	1.70	0.688	0.647
	MSE-SSMBA	0.588	2.20	0.579	0.520	0.941	1.39	0.738	0.711
	MSE-EDA	0.606	2.11	0.597	0.512	0.937	1.48	0.767	0.732
	MSE-BT	0.536	2.27	0.480	0.422	0.954	1.12	0.764	0.750
	MSE-Random	0.457	2.36	0.451	0.397	0.904	1.79	0.665	0.591
	ATC-NE	0.378	3.57	0.430	0.294	0.673	2.35	0.536	0.52
	ATC-MC	0.382	3.57	0.433	0.297	0.718	2.21	0.570	0.556

Table 6: Correlation metrics evaluating the quality of our smoothness measure on two tasks, sentiment analysis and natural language inference, and two architectures, CNN and RoBERTa. Details on metric calculations and baselines are provided in sections 3.3 and 4.4. This full table of results includes metrics calculated with our negative entropy smoothness measure as well.